Journal of Solid State Chemistry 184 (2011) 1387–1392

Contents lists available at ScienceDirect

Journal of Solid State Chemistry

journal homepage: www.elsevier.com/locate/jssc

New coordination polymers from 1D chain, 2D layer to 3D framework constructed from 1,2-phenylenediacetic acid and 1,3-bis(4-pyridyl)propane flexible ligands

Ling-Yun Xin, Guang-Zhen Liu *, Li-Ya Wang

College of Chemistry and Chemical Engineering, Luoyang Normal University, Luoyang 471022, PR China

ARTICLE INFO

Article history:
Received 31 December 2010
Received in revised form
30 March 2011
Accepted 3 April 2011
Available online 14 April 2011

Keywords:
Coordination polymer
Penetrated network
Flexible dicarboxylate
N-donor ligand
Fluorescent analysis

ABSTRACT

The hydrothermal reactions of Cd, Zn, or Cu(II) acetate salts with H_2PHDA and BPP flexible ligands afford three new coordination polymers, including $[Cd(PHDA)(BPP)(H_2O)]_n$ **(1)**, $[Zn(PHDA)(BPP)]_n$ **(2)**, and $[Cu_2(PHDA)_2(BPP)]_n$ **(3)** (H_2PHDA=1,2-phenylenediacetic acid, BPP=1,3-bis(4-pyridyl)propane). The single-crystal X-ray diffractions reveal that all three complexes feature various metal carboxylate subunits extended further by the BPP ligands to form a diverse range of structures, displaying a remarked structural sensitivity to metal(II) cation. Complex **1** containing PHDA-bridged binuclear cadmium generates 1D double-stranded chain, complex **2** results in 2D→2D interpenetrated (4,4) grids, and complex **3** displays a 3D self-penetrated framework with $4^8 6^6 8$ ***rob*** topology. In addition, fluorescent analyses show that both **1** and **2** exhibit intense blue-violet photoluminescence in the solid state.

1. Introduction

As an important branch in the field of supramolecular chemistry and crystal engineering, the design and assembly of metal–organic coordination frameworks (MOFs) have stimulated the interests of chemists over the past few decades [1–5], not only because of their intriguing network topologies [6], but also the possible application for such compounds in areas such as separation, catalysis, ion exchange, gas storage, etc. [7–10]. However, the effective and facile approach for the synthesis of such complexes is still the appropriate choice of well-designed organic ligands as linkers with metal ions or clusters as nodes due to their unclear formation mechanisms [11–14].

To date, most of the organic ligands used in MOFs chemistry are limited to a rigid aromatic carboxylate and/or a N-containing ligand [15–24], whereas the role of a flexible carboxylate ligand is somewhat ignored. Compared to rigid ligands, using flexible ones to construct coordination polymers seem more difficult and developing systematic methodologies of synthesis materials from prior design structure *via* flexible ligands are still a great challenge [25], which may be attributed to their unpredicted structures. However, flexible molecules can easily adjust their conformations to meet the coordination requirement of the metal ion [26–39] and may prone to promote helical or looped structural motifs through which other organic linkers can penetrate [40–45]. Thus, the flexibility of the ligand can afford a good opportunity to enrich the structural and functional diversities of MOFs and provide the further understanding of the directional synthesis of target coordination polymers. It is therefore an important aspect worthwhile paying attention to, and is the potential for erecting some signposts toward future research on predicted and pre-designed coordination polymers.

With these considerations in mind, our theme is the controllable synthesis of penetrated metal–organic networks by the use of flexible ligands. The simultaneous employment of conformationally flexible ligands such as phenylenediacetate (H_2PHDA) and 1,3-bis(4-pyridyl)-propane (BPP) could thus conceivably act in tandem to foster penetrated coordination polymer topologies. In this work, systematic studies have been carried out in our laboratory by the reaction of Cd, Zn, or Cu(II) acetate salts with the H_2PHDA and BPP flexible ligands, and producing three coordination complexes with the range of structural dimensionalities from 1D double-stranded chain, $Cd(PHDA)(BPP)(H_2O)]_n$ **(1)**, 2D→2D interpenetrated layer, $[Zn(PHDA)(BPP)]_n$ **(2)** to 3D self-penetrated framework, $[Cu_2(PHDA)_2(BPP)]_n$ **(3)**. The details of their synthesis condition, coordination structure, and luminescence are reported below.

2. Experimental

2.1. Materials and physical measurements

All reagents used in these syntheses were of analytical grade and used as purchased without further purification. Elemental analyses

* Corresponding author. Fax: +86 379 65511205.
E-mail address: gzliu@yahoo.com.cn (G.-Z. Liu).

0022-4596/$ - see front matter © 2011 Elsevier Inc. All rights reserved.
doi:10.1016/j.jssc.2011.04.002

(C, H, N) were performed on a Vario EL III elemental analyzer. Infrared spectra were recorded on a VECTOR-22 spectrophotometer within 400–4000 cm^{-1} using the samples prepared as pellets with KBr. Luminescence spectra were performed on a Hitachi F-4500 fluorescence spectrophotometer at room temperature.

2.2. Synthesis of $[Cd(PHDA)(BPP)(H_2O)]_n$ **(1)**

The mixtures of H_2PHDA (0.1 mmol, 19.4 mg), BBP (0.2 mmol, 39.7 mg), $Cd(OAC)_2 \cdot 2H_2O$ (0.1 mmol, 26.7 mg), NaOH (0.1 mmol), *N,N′*-dimethylformamide (DMF, 4.0 ml), and H_2O (4.0 ml) were placed in a 23 ml Teflon liner stainless steel reactor. The vessel was heated to 120 °C for 4 days, then cooled at 5 °C h^{-1} to room temperature. Colorless crystals were obtained, and further crystals were filtered off, washed with mother liquid, and dried under ambient conditions. Yield 53%. Elemental analysis calcd (%) for $C_{23}H_{24}CdN_2O_5$: C 53.04, H 4.64, N 5.38 Found: C 53.27, H 4.82, N 5.26.

2.3. Synthesis of $[Zn(PHDA)(BPP)]_n$ **(2)**

Compound **2** was synthesized in a similar way as that described for **1**, except that $Zn(OAC)_2 \cdot 2H_2O$(0.1 mmol, 21.9 mg) replaced the metal center. Yield 46%. Elemental analysis calcd (%) for $C_{23}H_{22}ZnN_2O_4$: C 60.61, H 4.86, N 6.14 Found: C 60.56, H 4.92, N 6.20.

2.4. Synthesis of $[Cu_2(PHDA)_2(BPP)]_n$ **(3)**

Compound **3** was prepared by using H_2PHDA (0.2 mmol, 38.8 mg), BBP (0.1 mmol, 19.8 mg), $Cu(OAC)_2 \cdot 2H_2O$ (0.1 mmol, 20.0 mg) and H_2O (8 ml) which were placed in a 23 ml Teflon liner stainless steel reactor. The vessel was heated to 120 °C for 4 days, then cooled at 5 °C h^{-1} to room temperature. Blue crystals were obtained and crystals were filtered off, washed with water liquid, and dried under ambient conditions. Yield 39%. Elemental analysis calcd (%) for $C_{16.5}H_{15}CuNO_4$: C 55.85, H 4.26, N 3.95 Found: C 55.88, H 4.32, N 3.89.

2.5. X-ray crystallography

Suitable single crystals of **1–3** were mounted on a Bruker Smart APEX II CCD diffractometer equipped with graphite-monochromated Mo *Ka* radiation (λ=0.071073 nm) by using Φ/ω scan technique at room temperature. Semi-empirical absorption corrections were applied using SADABS. The structures were solved using direct method and refined by full-matrix least-squares on F^2. All non-hydrogen atoms were refined anisotropically, and hydrogen atoms were located from the difference map, and then added geometrically. All calculations were performed using the *SHELXTL-97* program package [46–48]. Crystal data and experimental details for compounds **1–3** are presented in Table 1. Selected bond distances and angles are listed in Table S1.

3. Result and discussion

3.1. Synthesis and IR characterization

Hydrothermal method has been extensively explored as an effective and powerful tool in the self-assembly of MOFs, although the mechanism is not completely clear so far [49]. As is known, there are a variety of parameters such as the pH value, temperature, the molar ratio of the reactant and reactant solvent, which can exert a profound influence on the final reaction outcome. In our experiment, the hydrothermal reactions of compound **1–3** were carried out in different solvent, the molar ratio, and pH values. It was found that the compound **1** and **2** may be the favored products with adding the 0.1 mmol NaOH and DMF as the solvent (DMF:H_2O=1:1), which proved the **1** and **2** seem sensitive to the pH value and solvent. However, the compound **3** was produced in aqueous solution without the NaOH.

The IR spectra of **1–3** show the sharp characteristic bands of dicarboxylate groups in the usual region at 1613–1630 and 1485–1500 cm^{-1} for the asymmetric stretching and the 1363–1393 cm^{-1} for the symmetric stretching. Features corresponding to pyridyl ring puckering mechanisms are evident in the region 850 and 600 cm^{-1}. The broad bands in the area of ~3400–3200 cm^{-1} in compound **2** belong to the O–H stretching

Table 1
Crystal data and structure refinement parameters for **1–3**.

	1	**2**	3
Empirical formula	$C_{23}H_{24}CdN_2O_5$	$C_{23}H_{22}ZnN_2O_4$	$C_{16.5}H_{15}CuNO_4$
Formula weight	520.84	455.80	354.83
Temperature (*K*)	296(2)	296(2)	296(2)
Crystal system	Triclinic	Monoclinic	Orthorhombic
Space group	*P*−1	*P*2(1)/*c*	*Pccn*
a (Å)	12.5326(11)	10.4461(13)	11.753(4)
b (Å)	13.1476(12)	16.919(2)	28.513(10)
c (Å)	14.7948(13)	12.3974(15)	9.064(3)
a (deg.)	75.6240 (10)	90.00	90.00
β (deg.)	70.8980(10)	110.7200(10)	90.00
γ (deg.)	87.1140(10)	90.00	90.00
Volume ($Å^3$)	2230.2(3)	2049.4(4)	3037.7(18)
Crystal size (mm)	0.23 × 0.21 × 0.19	0.39 × 0.38 × 0.27	0.21 × 0.06 × 0.05
Z	4	4	8
D_{calc} (g cm^{-3})	1.551	1.477	1.552
μ (mm^{-1})	1.015	1.231	1.456
F(0 0 0)	1056	944	1456
θ range (deg.)	2.39 to 25.50	2.41 to 25.50	2.76 to 25.50
Reflections collected	17124	12927	21298
Independent reflections	8236 [*R*(int)=0.0181]	3765 [*R*(int)=0.0243]	2822 [*R*(int)=0.1221]
Data/restraints/parameters	8236/0/559	3765/0/271	2822/0/204
Goodness-of-fit	1.080	1.045	1.021
Final *R* indices [$I > 2\sigma(I)$]	R_1=0.0360, ωR_2=0.0973	R_1=0.0291, ωR_2=0.0718	R_1=0.0559, ωR_2=0.1153
R indices (all data)	R_1=0.0468, ωR_2=0.1023	R_1=0.0399, ωR_2=0.0782	R_1=0.1017, ωR_2=0.1281

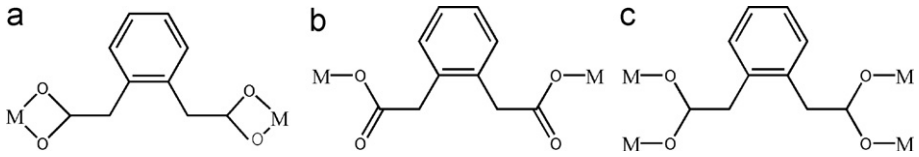

Scheme 1. Coordination modes of PHDA observed in complexes **1–3**.

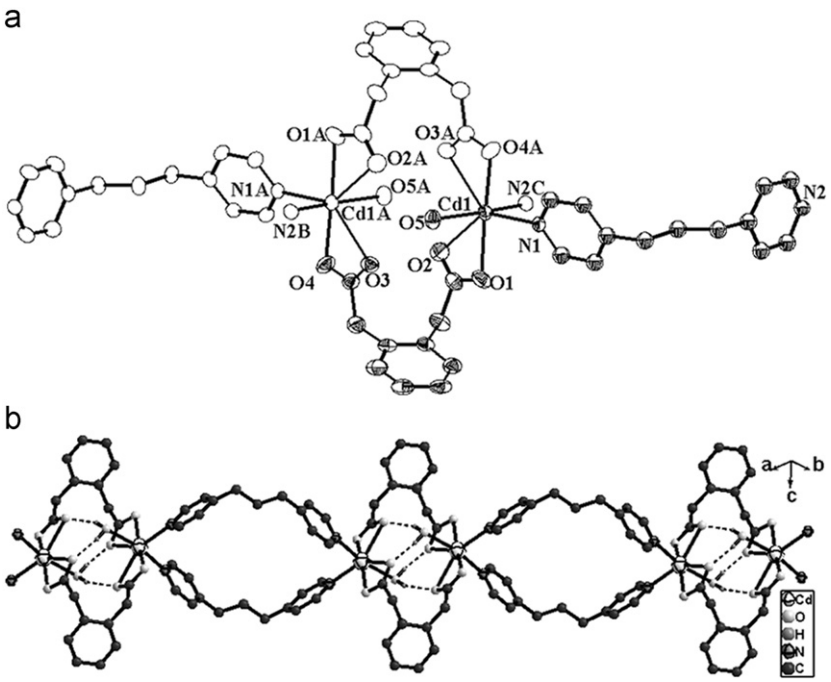

Fig. 1. (a) Coordination environment of the dinuclear cadmium unit in **1**. Symmetry codes: A, $-x$, $1-y$, $1-z$; B, $-1+x$, $1+y$, z; C, $1-x$, $-y$, $1-z$. (b) The dinuclear cadmium connected by BBP ligands to form a 1D double-stranded chain.

modes within coordinated water molecules. No peak of compound **1–3** in $\sim$1680–1700 cm^{-1} demonstrates complete deprotonation of the H_2PHDA after forming the coordination polymers. Various coordination modes of PHDA ligand in **1–3** are shown in Scheme 1.

3.2. Structural description of $[Cd(PHDA)(BPP)(H_2O)]_n$ (1)

Single-crystal X-ray analysis shows the asymmetric unit of compound **1** contains two crystallographically independent molecule fragments with almost uniform configuration (Fig. S1). So, only one of molecule fragments is discussed below (Fig. 1(a)). Each molecule fragment includes one crystallographically separate Cd atom, one PHDA dianion, one BBP ligand, and one ligated water molecule. The Cd atom displays a highly distorted pentagonal bipyramid with four oxygen atoms from two chelating carboxylate group belonging to different PHDA molecules (Cd–O: 2.323(3)Å–2.600(3) Å), two nitrogen atoms from BBP ligands (Cd–N: 2.346(3) Å and 2.369(3) Å), and one ligated water molecule (Cd–O: 2.351(2) Å).

The symmetry-related two cadmium atoms are connected by a pair of PHDA anions via a $\mu_1-\eta^1{:}\eta^1$ (Scheme 1a) coordination mode to form a binuclear cadmium unit with the Cd … Cd distance of 5.3251 Å. Extension of the structure through the two pairs of bisymmetric BBP molecules results in a one-dimensional double-stranded chain running along the [1 -1 0] crystal direction, as shown in Fig. 1(b). There exist H-bonds between ligated water molecules and oxygen atoms in PHDA within each binuclear unit with O–O distances from 2.752(4) to 2.839(4) Å (Fig. 1(b)). The detailed hydrogen bond parameters are listed in Table S2. The adjacent 1D chains are stacked in a parallel fashion and cohered together by the weak effect of van der Waals force into the entire 3D supramolecular network of complex **1**.

3.3. Structural description of $[Zn(PHDA)(BPP)]_n$ (2)

The asymmetric unit (Fig. 2a) of compound **2** contains one crystallographically independent Zn(II) atom, one PHDA anion, and one BPP molecule. The Zn(II) atom is coordinated by two carboxylate oxygen atoms from two different PHDA ligand adopting a $\mu_1-\eta^1{:}\eta^0$ (Scheme 1b) bridging coordination mode and two nitrogen atom from two different BPP molecules to form a distorted tetrahedral geometry. The Zn–O bond lengths are 1.9511(15) and 1.9529(16) Å, and Zn–N bond lengths are 2.0324(18) and 2.0477(18) Å.

Along the crystallographic *b* axis, the PHDA ligands bridge the Zn(II) centers to form zigzag carboxylate chains, which are interconnected to each other through the BPP molecules to result in a (4,4) grid layer (Fig. 2(b)). Each layer is corrugated with two BPP ligands, two PHDA ligands, and four Zn atoms forming a repeating rhombic grid with a side length of 12.3974\9.4542 A° and a diagonal measurement of 17.6363\13.2332 A° based on the metal–metal distances. In order to minimize the presence of large cavities and to stabilize the framework during the assembly process, the corrugated nature and larger cavities for each layer can permit two adjacent layers interpenetrate each other to

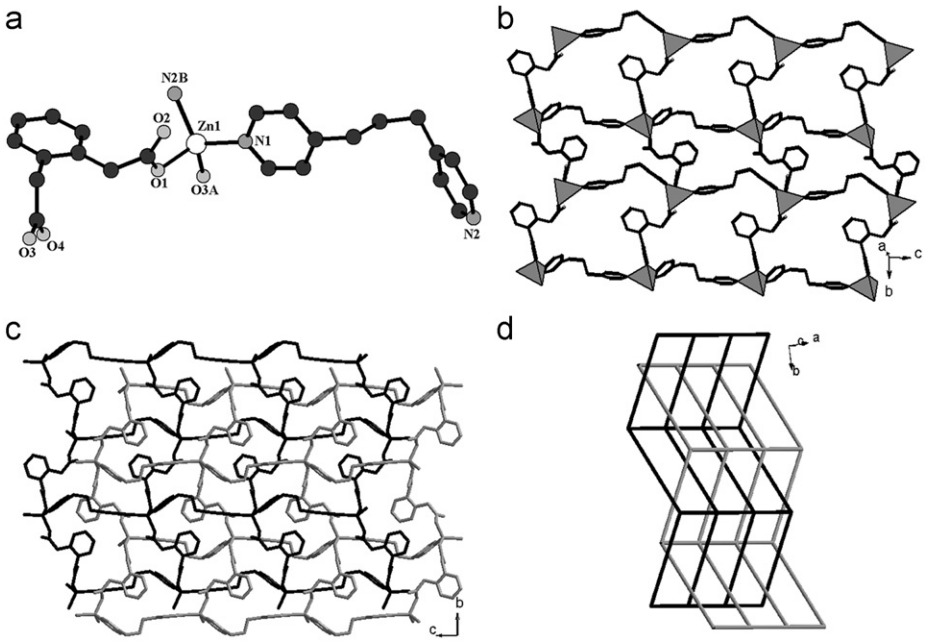

Fig. 2. (a) Coordination environment of the zinc unit in **2**. Symmetry codes: A, $-x$, $-0.5+y$, $0.5-z$; B, x, y, $0.5-z$. (b) The zinc clusters connected by PHDA and BPP ligands to form a 2D (4, 4) grid. (c) The interpenetrated 2D layers. (d) Topology of **2** displaying 2D→2D interpenetration.

weave into a twofold interpenetrating structure (Fig. 2(c) and Fig. S2), which may be attributed to the backbone flexibility of PHDA and BPP ligands. Thus, the pronounced structural feature is that **2** represents a 2D→2D interpenetrated network (Fig. 2(d)). The adjacent interpenetrated networks are stacked in a parallel fashion and cohered together by the weak effect of van der Waals force to form the entire 3D supramolecular network of complex **2**.

3.4. Structural description of $[Cu_2(PHDA)_2(BPP)]_n$(3)

The asymmetric unit of **3** contains one crystallographically distinct Cu(II) atom, one PHDA anion and one half BPP molecule (Fig. 3(a)). The Cu(II) center adopts a distorted square-pyramidal coordination environment, in which four oxygen atoms from carboxyl groups belonging to different PHDA anions occupy the equatorial plane and one nitrogen atoms from BPP molecules occupy the axial position. The Cu–O bond lengths are in the range of 1.966(3)–1.979(3) Å and the Cu–N bond lengths is 2.156(4) Å.

The symmetry-related two Cu atoms are cohered together by the carboxyl groups of PHDA anions by a $\mu_2-\eta^1{:}\eta^1$ mode (Scheme 1c) to form the $\{Cu_2(COO)_4\}$ paddlewheel units with the Cu…Cu distance of 2.6333(10) Å, which are further connected through the full length of the PHDA ligands constructing $[Cu(PHDA)]_n$ carboxylate layer subunit that lies parallel to the *ac* crystal plane (Fig. 3(b)). Within the layer, each $\{Cu_2(COO)_4\}$ paddlewheel unit is connected to four adjacent ones in a rhomboid grid (4,4) manner. The parallel $[Cu(PHDA)]_n$ layer are pillared to each other by gauche-anticonformation BPP tethers to build a $[Cu_2(PHDA)_2(BPP)]_n$ 3-D coordination polymer lattice (Fig. 3(c)).

Topologically, the Cu dimers can be regarded as the network nodes. These are linked in two dimensions by the PHDA ligands, to give (4,4) sheets, and in the third dimension by pairs of BPP ligands acting as single bridges. For each cluster, one pair of BPP ligands bridges to the sheet above, and another ones bridge to the sheet below, making the Cu dimers six-connecting nodes. The BPP bridges, however, are slanted rather than perpendicular to the sheets and crisscross in two different directions (Fig. 3(e)). Thus, the usual ***R-Po*** net is not formed, but rather an unusual six-connected net with $(4^8 6^6 8)$ ***rob*** network topology is formed (Fig. 3(d)). This net is self-penetrating, that is, there are six-membered shortest circuits that are penetrated by rods of the same net. A close-up network perspective view of the self-penetration of the BPP linkers through six-membered rings in the lattice is depicted in Fig. S3. The self-assembly of the $\{Cu_2(COO)_4\}$ paddle-wheel clusters in **3** can provide the impetus for generation of the 6-connected 3-D lattice, with self-penetration of the BPP ligands fostered by the tilted orientation of the apical positions at the square pyramidal copper coordination spheres.

3.5. Fluorescent properties of *1* and *2*

Inorganic–organic hybrid coordination polymers, especially those with d^{10} metal centers, have been investigated for photoluminescent properties and for potential applications as fluorescence-emitting materials, such as light-emitting diodes (LEDS). The solid-state fluorescence spectra of PHDA, **1**, and **2** at room temperature have been determined, as shown in Fig. 4. It is shown that complex **1** has a maximum emission at 375 nm and **2** displays a strong emission at 376 nm. These emissions are assigned to the intraligand $\pi-\pi*$ fluorescence emission since the corresponding PHDA ligand also shows a similar maximum emission at 370 nm [50–53]. In addition, fluorescent spectra of **1** and **2** have more intensity at longer wavelength compared to free PHDA ligand. Although more detailed theoretical and spectroscopic studies may be necessary for better understanding of the luminescent mechanism [54,55], the strong fluorescence emissions of those complexes make them potentially useful photoactive materials.

4. Conclusions

We have presented the synthesis and structure of three new coordination polymers assembled from H_2PHDA with pendant arms and flexible BPP molecule under hydrothermal conditions. Their structures show a varieties of supramolecular networks from 1D double-stranded chain, 2D→2D interpenetrated (4,4) grid layer to 3D self-penetrated framework, showing a remarked

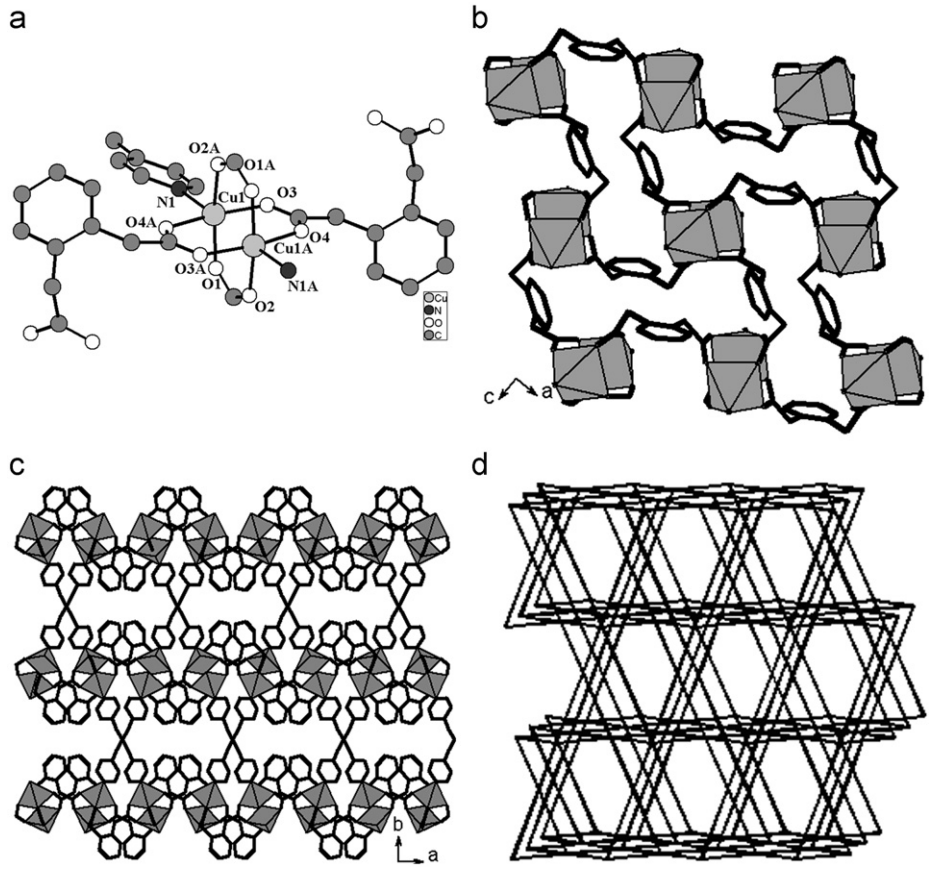

Fig. 3. (a) Coordination environment of the dinuclear copper unit in **3**. Symmetry codes: A, $-x, 1-y, -z$; B, $-0.5+x, 1-y, 0.5-z$; C, $0.5-x, y, -0.5+z$. (b) The copper clusters connected by PHDA to form a 2D layer. (c) Containing paddle-wheel layers connected by BPP to form 3D network. (d) 3D self-penetrating 6-connected ($4^8.6^6.8$) network topology.

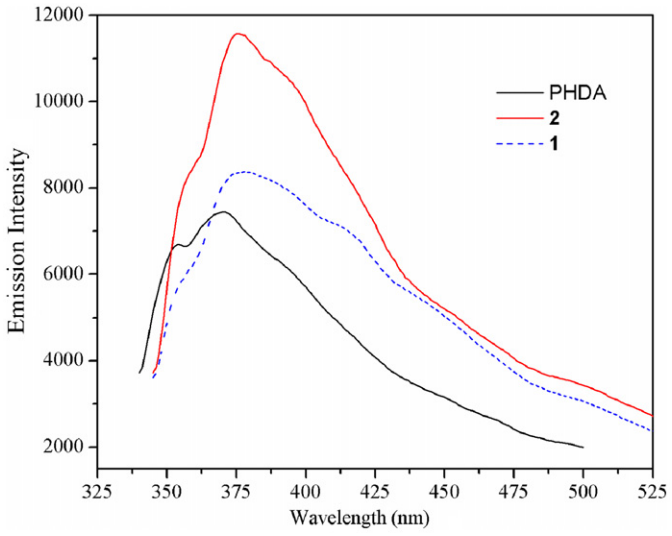

Fig. 4. Emission spectra of compound **1** and **2** compared to free PHDA ligands.

structure sensitivity to metal(II) center with different coordination geometries. It is found that the PH value and different solvent of the reactive system play an important role to form the crystalloid. Fluorescent analyses of 1 and 2 show the enhancement of luminescence in the longer wavelength compared to that of free PHDA ligand.

Acknowledgments

This work was supported by the National Natural Science Foundation of China (Nos. 20971064 and 21071074) and the Foundation of Education Committee of Henan Province (No. 092102210315).

Appendix A. Supporting information

Supplementary data associated with this article can be found in the online version at doi:10.1016/j.jssc.2011.04.002.

References

[1] X. Zhu, J.W. Zhao, B.L. Li, Y. Song, Y.M. Zhang, Y. Zhang, Inorg. Chem. 49 (2010) 1266.
[2] L.F. Ma, L.Y. Wang, S.H. Chen, H.W. Hou, S.R. Batten, Polyhedron 28 (2009) 2494.
[3] J.L.C. Rowsell, O.M. Yaghi, J. Am. Chem. Soc. 128 (2006) 1304.
[4] T.L. Hu, R.Q. Zou, J.R. Li, X.H. Bu, Dalton Trans. (2008) 1302.
[5] M. Wang, M.H. Xie, C.D. Wu, Y.G. Wang, Chem. Commun. (2009) 2396.
[6] O.M. Yaghi, M. O'Keeffe, M. Kanatzidis, J. Solid State Chem. 152 (2000) 1.
[7] S. Noro, R. Kitaura, M. Kondo, S. Kitagawa, T. Ishii, H. Matsuzaka, M. Yamashita, J. Am. Chem. Soc. 124 (2002) 2568.
[8] L. Carlucci, G. Ciani, D.M. Proserpio, Coord. Chem. Rev. 246 (2003) 247.
[9] L. Brammer, Chem. Soc. Rev. 33 (2004) 476.
[10] R. Matsuda, R. Kitaura, S. Kitagawa, Y. Kubota, R.V. Belosludov, T.C. Kobayashi, H. Sakamoto, T. Chiba, M. Takata, Y. Kawazoe, Y. Mita, Nature 436 (2005) 238.
[11] X.G. Liu, J. Huang, S.S. Bao, Y.Z. Li, L.M. Zheng, Dalton Trans. (2009) 9837.

[12] H. Ren, T.Y. Song, J.N. Xu, S.B. Jing, Y. Yu, P. Zhang, L.R. Zhang, Cryst. Growth Des. 9 (2009) 105.
[13] M.H. Zeng, Y.L. Zhou, M.C. Wu, H.L. Sun, M. Du, Inorg. Chem. 49 (2010) 6436.
[14] P. Pachfule, T. Panda, C. Dey, R. Banerjee, CrystEngComm 12 (2010) 2381.
[15] M.A. Braverman, R.J. Staples, R.M. Supkowski, R.L. LaDuca, Ployhedron 27 (2008) 2291.
[16] P.J. Stang, B.A. Olenyuk, Chem. Res. 30 (1997) 502.
[17] Z. Ni, A Yassar, T. Antoun, O.M. Yaghi, J. Am. Chem. Soc. 127 (2005) 12752.
[18] H. Furukawa, J. Kim, K.E. Plass, O.M. Yaghi, J. Am. Chem. Soc. 128 (2006) 8398.
[19] B. Moulton, J. Lu, A. Mondal, M.J. Zaworotko, Chem. Commun. (2001) 863.
[20] F.M. Tabellion, S.R. Seidel, A.M. Arif, P.J. Stang, Angew. Chem. Int. Ed. 40 (2001) 1529.
[21] L. Pan, E.B. Woodlock, X. Wang, K.C. Lam, A.L. Rheingold, Chem. Commun. (2001) 1762.
[22] M.L. Tong, Y.M. Wu, J. Ru, X.M. Chen, H.C. Chang, S. Kitagawa, Inorg. Chem. 41 (2002) 4846.
[23] W.J. Zhuang, X.J. Zheng, L.C. Li, D.Z. Liao, H. Ma, L.P. Jin, CrystEngComm 9 (2007) 653.
[24] Z.Z. Lin, F.L. Jiang, D.Q. Yuan, L. Chen, Y.F. Zhou, M.C. Hong, Eur. J. Inorg. Chem. (2005) 1927.
[25] T.F. Liu, J. Lü, R. Cao, CrystEngComm 12 (2010) 660.
[26] K. Uemura, R. Matsuda, S. Kitagawa, J. Solid State Chem. 178 (2005) 2420.
[27] Z.H. Zhang, Z.L. Shen, T. Okamura, H.F. Zhu, W.Y. Sun, N. Ueyama, Cryst. Growth Des. 5 (2005) 1191.
[28] H.F. Zhu, J. Fan, T. Okamura, Z.H. Zhang, G.X. Liu, K.B. Yu, W.Y. Sun, N. Ueyama, Inorg. Chem. 45 (2006) 3941.
[29] H.F. Zhu, W.Y. Sun, T. Okamura, N. Ueyama, Inorg. Chem. Commun. 6 (2003) 168.
[30] G.X. Liu, Y.Q. Huang, Q. Chu, T.A. Okamura, W.Y. Sun, H. Liang, N. Ueyama, Cryst. Growth Des. 8 (2008) 3233.
[31] S. Zang, Y. Su, Y. Li, Z. Ni, Q. Meng, Inorg. Chem. 45 (2006) 174.
[32] L. Wang, M. Yang, G. Li, Z. Shi, S. Feng, Inorg. Chem. 45 (2006) 2474.
[33] S. Wang, Y. Hou, E. Wang, Y. Li, L. Xu, J. Peng, S. Liu, C. Hu, New J. Chem. 27 (2003) 1144.
[34] M.A. Braverman, R.L. LaDuca, Cryst. Growth Des. 7 (2007) 2343.
[35] F.N. Dai, J.M. Dou, H.Y. He, X.L. Zhao, D.F. Sun, Inorg. Chem. 49 (2010) 4117.
[36] L. Pan, K.M. Adams, H.E. Hernandez, X. Wang, C. Zheng, Y. Hattori, K. Kaneko, J. Am. Chem. Soc. 125 (2003) 3062.
[37] O. Fabelo, J. Pasan, L.C. Delgado, F.S. Delgado, F. Lloret, M. Julve, C.R. Perez, Inorg. Chem. 48 (2009) 6086.
[38] T. Liu, J. Lu, L. Shi, Z. Guo, R. Cao, CrystEngComm 11 (2009) 583.
[39] A.D. Burrows, R.W. Harrington, M.F. Mahon, S.J. Teat, Eur. J. Inorg. Chem. (2003) 766.
[40] S.Y. Yao, Y.Q. Tian, CrystEngComm 12 (2010) 697.
[41] P.K. Chen, Y. Qi, Y.X Che, J.M. Zheng, CrystEngComm 12 (2010) 720.
[42] J. Yang, J.F. Ma, S.R. Batten, Z.M. Su, Chem. Commun. (2008) 2233.
[43] X.D. Zheng, T.B. Lu, CrystEngComm 12 (2010) 324.
[44] L.K. Sposato, J.A. Nettleman, R.L. LaDuca, CrystEngComm 12 (2010) 2374.
[45] M. Zhang, D. Li, J. Wang, F. Fu, M. Du, K. Zou, X. Gao, Dalton Trans. (2009) 5355.
[46] GM Sheldrick, SHELXS-97, Program for X-ray Crystal Structure Determination, Göttingen University, Germany, 1997.
[47] GM Sheldrick, SHELXL-97, Program for X-ray Crystal Structure Refinement, Göttingen University, Germany, 1997.
[48] GM Sheldrick, SHELXTL, Version V, Siemens Industrial Automation Inc, Madison, Wisconsin, U.S.A, 1997.
[49] L.F. Ma, B. Liu, L.Y. Wang, C.P. Li, M. Du, Dalton Trans. 39 (2010) 2301.
[50] D.R. Xiao, R. Yuan, Y.Q. Chai, E.B. Wang, Eur. J. Inorg. Chem. (2008) 2610.
[51] J. Tao, M.L. Tong, J.X. Shi, X.M. Chen, S.W. Ng, Chem. Commun. (2000) 2043.
[52] L.F. Ma, B. Li, X.Y. Sun, L.Y. Wang, Y.T. Fan, Z. Anorg. Allg. Chem. 636 (2010) 1606.
[53] F.Y. Lian, F.L. Jiang, D.Q. Yuan, J.T. Chen, M.Y. Wu, M.C. Hong, CrystEngComm 10 (2008) 905.
[54] A.R. Diéguez, A.S. Castillo, A. Sironi, J.M. Seco, E. Colacio, CrystEngComm 12 (2010) 1876.
[55] H.Y. Bai, J.F. Ma, J. Yang, L.P. Zhang, J.C. Ma, Y.Y. Liu, Cryst. Growth Des. 10 (2010) 1946.